Dispersion relation of the ρ meson in hot and dense nuclear matter

Ji-sheng Chen[a] Jia-rong Li[b] Peng-fei Zhuang[a]
[a] *Physics Department, Tsinghua University, Beijing 100084, People's Republic of China*
[b] *Institute of Particle Physics, Hua-Zhong Normal University, Wuhan 430079, People's Republic of China*

The dispersion relation of ρ meson in both timelike and spacelike regimes in hot and dense nuclear medium is analyzed and compared with σ meson based on the quantum hadrodynamics model. The pole and screening masses of ρ and σ are discussed. The behavior of screening mass of ρ is different from that of σ due to different Dirac- and Fermi-sea contributions at finite temperature and density.

PACS numbers: 14.40.Cs, 11.55.Fv, 11.10.Wx

arXiv:nucl-th/0209043v4 31 Jul 2003

Heavy-ion collision physics has stimulated intense investigations of the properties of strongly interacting, hot and dense nuclear matter[1]. Among the proposed signals for detecting quark-hadron phase transition, dileptons and photons are considered to be the clearest ones because they can penetrate the medium almost undisturbed and reflect the property of the fireball formed in the initial stage of collisions[2]. Furthermore, the dileptons from the decay of light vector mesons can be considered as possible signals of the partial chiral symmetry restoration. Especially, the property of ρ in hot and dense environment has attracted much attention in the literature due to its relatively larger decay width compared with ω and ϕ[3, 4, 5]. It is interesting that the ρ mass decreasing mechanism can be used to explain the low invariant mass dilepton enhancement in central $A-A$ collisions observed by CERES-NA45[6, 7, 8].

From the point of view of many-body theory, the collective effect of medium on a meson is reflected by its full propagator, which determines its dispersion relation as well as the response to the external source[9, 10, 11]. Due to the broken Lorentz symmetry, the dispersion relations for longitudinal and transverse modes of vector mesons are different. However, the timelike and spacelike regimes are related to each other through the dispersion relation as in the case of QED[12]. With vector meson dominance model, the ρ meson screening mass is an important quantity related to the EM (electromagnetic) Debye mass and to the emissivity of dileptons and photons produced in heavy-ion collisions. For example, the screening mass in spacelike limit is associated with the isospin fluctuations which can be used as a potential signature of QGP (quark-gluon plasma) formation[13]. Furthermore, the scalar quark density fluctuation of QCD is related to the spacelike limit of in-medium self-energy of σ as pointed out in Ref.[14], where the contribution of free nucleons at $T = 0$ is analyzed through one-loop NN^{-1} excitation. In Refs. [15, 16], it was found that the Dirac-sea contribution to the pole mass of ρ dominates over Fermi sea's. In this paper, we discuss the dispersion relations of ρ and σ in both spacelike and timelike regimes determined by the pole positions of their in-medium propagators. The medium effects on ρ and σ at finite temperature T and baryon density ρ_B are taken into account in the framework of quantum hadrodynamics model(QHD) through the in-medium nucleon excitation.

We start from QHD-I to obtain the effective nucleon mass M_N^* and effective chemical potential μ^* for discussing the in-medium meson property. In the relativistic Hartree approximation, the self-consistent equations for M_N^* and μ^* can be written as [16, 17]

$$\begin{aligned} M_N^* - M_N = &-\frac{g_\sigma^2}{m_\sigma^2}\frac{4}{(2\pi)^3}\int d^3\mathbf{p}\frac{M_N^*}{\omega}\left[n_B + \bar{n}_B\right] \\ &+ \frac{g_\sigma^2}{m_\sigma^2}\frac{1}{\pi^2}\left[M_N^{*3}\ln\left(\frac{M_N^*}{M_N}\right) - M_N^2(M_N^* - M_N)\right. \\ &\left. - \frac{5}{2}M_N(M_N^* - M_N)^2 - \frac{11}{6}(M_N^* - M_N)^3\right], \quad (1) \\ \mu^* - \mu = &-g_\omega^2\rho_B/m_\omega^2, \quad (2) \end{aligned}$$

where $\omega = \sqrt{M_N^{*\,2} + p^2}$ is the nucleon energy and the baryon density ρ_B is defined by

$$\rho_B = \frac{4}{(2\pi)^3}\int d^3\mathbf{p}\left[n_B - \bar{n}_B\right], \quad (3)$$

with $n_B(\bar{n}_B)$ being the Fermi-Dirac distribution functions for (anti-)baryons, respectively. The coupled equations can be solved numerically with the parameters determined by fitting the binding energy at normal nuclear density ρ_0 given in Table.I. The M_N^* decreases with increasing density ρ_B at fixed temperature(see Fig.1), analogously to the result of mean field theory neglecting the vacuum fluctuations[16]. The effective chemical potential μ^* will affect the properties of mesons indirectly through the distribution functions.

In Minkowski space, the polarization tensor $\Pi^{\mu\nu}(k)$ of ρ can be divided into two parts with the standard projection tensors $P_L^{\mu\nu}$ and $P_T^{\mu\nu}$ according to

$$\Pi^{\mu\nu}(k) = \Pi_L(k)P_L^{\mu\nu} + \Pi_T(k)P_T^{\mu\nu} \quad (4)$$

with

$$\Pi_L(k) = \frac{k^2}{\mathbf{k}^2}\Pi^{00}(k), \qquad \Pi_T(k) = \frac{1}{2}P_T^{ij}\Pi_{ij}(k). \quad (5)$$

With the effective Lagrangian for ρNN interactions[18]

$$\mathcal{L}_{\rho NN} = g_{\rho NN}\left(\bar{\Psi}\gamma_\mu\tau^a\Psi V_a^\mu - \frac{\kappa_\rho}{2M_N}\bar{\Psi}\sigma_{\mu\nu}\tau^a\Psi\partial^\nu V_a^\mu\right),$$

where V_a^μ is the ρ meson field and Ψ the nucleon field, the polarization tensor is given in random phase approximation (RPA) by

$$\Pi^{\mu\nu}(k) = 2g_{\rho NN}^2 T \sum_{p_0} \int \frac{d^3\mathbf{p}}{(2\pi)^3} \mathrm{Tr}\left[\Gamma^\mu(k)\frac{1}{\not{p} - M_N^*}\Gamma^\nu(-k)\frac{1}{(\not{p}-\not{k}) - M_N^*}\right], \quad (6)$$

with $\Gamma^\mu = \gamma^\mu + (ik_\rho/2M_N)\sigma^{\mu\nu}k_\nu$. The temperature and effective chemical potential are hidden in the zero-component of nucleon momentum via $p_0 = (2n+1)\pi T i + \mu^*$. With the residue theorem, one can separate the polarization tensor into two parts

$$\Pi^{\mu\nu}(k) = \Pi_F^{\mu\nu}(k) + \Pi_D^{\mu\nu}(k), \quad (7)$$

where $\Pi_F^{\mu\nu}(k)$ corresponds to the particle-antiparticle contribution of the Dirac sea at $T = 0$ and $\Pi_D^{\mu\nu}(k)$ arises from the particle-hole contribution[19, 20, 21]. The various components of $\Pi_D^{\mu\nu}(k)$ are listed in the appendix and $\Pi_F^{\mu\nu}(k)$ can be found in Ref.[16].

For vector meson excitation in the medium, the dispersion relations determined by the pole positions of the full propagator $D^{\mu\nu}$ for longitudinal and transverse branches are different, while the pole masses determined by taking the limit $\Pi_{L,T}(k_0, |\mathbf{k}| \to 0)$ for L and T modes are consistent[16]. As pointed out in Ref.[13], the screening mass determined by $\Pi_L(0, |\mathbf{k}| \to 0)$ can be related to the isospin fluctuations. In general case including the Dirac sea contribution and the vacuum mass m_ρ, the screening masses are defined by the pole positions of full propagators related with the finite momentum self-energy $\Pi(0, \mathbf{k})$[12, 15]

$$\mathbf{k}^2 + m_\rho^2 + \Pi_{L,T}(0, \mathbf{k}) = 0. \quad (8)$$

The screening (Debye) masses $M_D = -i|\mathbf{k}|$ are the inverse Debye screening lengths and reflect the collective effects of medium, i.e., the damping characteristic $e^{-|\mathbf{k}|x}$ of the excitations with purely imaginary wave numbers. The self-consistent numerical results for M_D determined by (8) are indicated in Fig.1, where the effective nucleon mass M_N^* and the effective pole mass of ρ are also shown for comparison.

It is interesting to discuss the in-medium property of scalar meson σ with QHD and compare it with the vector mesons. At zero temperature, the property of σ has been discussed in Refs. [22, 23]. As pointed out in the introduction, the screening mass of σ in spacelike limit has been discussed at zero temperature by considering the one-loop NN^{-1} excitation with free nucleon gas[14]. At finite temperature, the σ meson self-energy with RPA is

$$\Pi_\sigma(k) = 2g_\sigma^2 T \sum_{p_0} \int \frac{d^3\mathbf{p}}{(2\pi)^3} \mathrm{Tr}\left[\frac{1}{\not{p} - M_N^*}\frac{1}{(\not{p}-\not{k}) - M_N^*}\right],$$

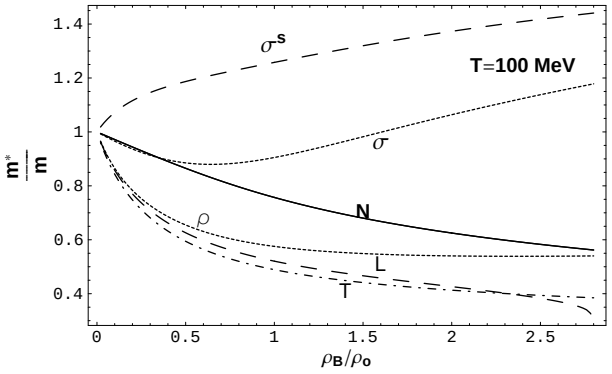

FIG. 1: Effective masses as functions of scaled density at temperature $T = 100$ MeV. The solid line represents the effective nucleon mass(labeled as N). The dotted lines are for pole masses(ρ and σ, respectively), dot-dashed for transverse screening mass (T). The dashed lines indicate the longitudinal screening mass(L) of ρ and screening mass(σ^s) of σ, respectively.

which can be reduced to

$$\Pi_\sigma(k) = \frac{3g_\sigma^2}{2\pi^2}\Big[3M_N^{*^2} - 4M_N^* M_N + M_N^2 - (M_N^{*^2} - M_N^2)\int_0^1 \ln\frac{M_N^{*^2} - x(1-x)k^2}{M_N^2}dx - \int_0^1 (M_N^2 - x(1-x)k^2)\ln\frac{M_N^{*^2} - x(1-x)k^2}{M_N^2 - x(1-x)k^2}dx\Big] + \frac{g_\sigma^2}{\pi^2}\int\frac{p^2dp}{\omega}(n_B + \bar{n}_B)\left[2 + \frac{k^2 - 4M_N^{*^2}}{4p|\mathbf{k}|}(a+b)\right], \quad (9)$$

where

$$a = \ln\frac{k^2 - 2p|\mathbf{k}| - 2k_0\omega}{k^2 + 2p|\mathbf{k}| - 2k_0\omega}, \quad b = \ln\frac{k^2 - 2p|\mathbf{k}| + 2k_0\omega}{k^2 + 2p|\mathbf{k}| + 2k_0\omega}$$

with $k^2 = k_0^2 - \mathbf{k}^2$. It is neccesary to note again that here we discuss the full propagator D_σ with the in-medium nucleons. The effective masses of σ meson defined analogously to those of ρ are also displayed in Fig.1.

The pole masses m_ρ^*, M_N^* and m_σ^* venus ρ_B at fixed T behave very differently. The effective nucleon mass decreases monotonously with increasing density, while the effective pole mass of ρ decreases at first and then becomes saturated. The pole mass m_σ^* also decreases in the low density region. As for the screening mass behavior, the longitudinal and transverse Debye ones of ρ decrease, but the one of σ increases with increasing density.

The corresponding dispersion relation curves calculated from the pole position of the full propagator $D^{\mu\nu}$ in both timelike and spacelike regions for ρ are shown in the upper panel of Fig.2. Due to the tensor(magnetic) coupling and the relatively smaller coupling constant $g_{\rho NN}$ compared with ω meson, the invariant in-medium mass $M_\rho = \sqrt{k_0^2 - \mathbf{k}^2}$ is almost a constant in the timelike region. The dispersion relation curves for the longitudinal

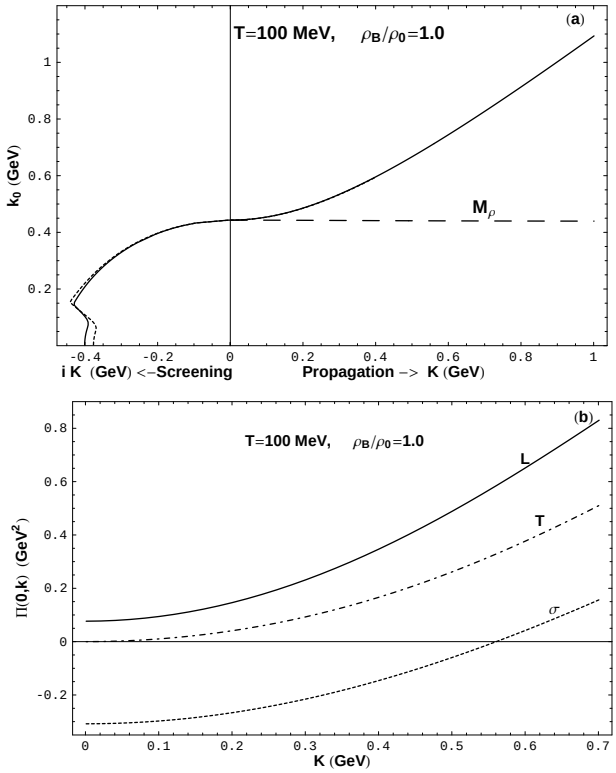

FIG. 2: (a) Dispersion relation curves for ρ. The solid line corresponds to L mode, dot-dashed to T mode and long-dashed to invariant mass $M_\rho = \sqrt{k_0^2 - \mathbf{k}^2}$; (b) $\Pi(0, \mathbf{k})$ for ρ and σ. The solid line and dot-dashed lines correspond respectively to L and T modes of ρ, and the dotted line is for σ.

and transverse branches almost coincide and can only be separated from each other in the spacelike screening region. For comparison, the spacelike tensors $\Pi(0, \mathbf{k})$ of ρ and σ are shown in the lower panel of Fig.2. For ρ, in the limit $|\mathbf{k}| \to 0$ the Dirac-sea and the tensor coupling contributions vanish, and the Fermi sea contributes only to the longitudinal mode. Therefore, the screening mass determined by the spacelike limit of $\Pi(0, \mathbf{k})$ will be very different from what we showed in Fig.1. The difference between the L and T modes dominated by the Fermi-sea contribution increases with increasing momentum $K = |\mathbf{k}|$. For σ, $\Pi(0, \mathbf{k})$ contains both Dirac- and Fermi-sea contributions in the spacelike limit. It is the Fermi-sea contribution which leads to a negative $\Pi(0, \mathbf{k})$ in the low $|\mathbf{k}|$ region.

In summary, we have analyzed the dispersion relations of ρ and σ in hot and dense nuclear environment in the framework of QHD in timelike and spacelike regimes. The pole and screening masses of ρ are found to decrease with increasing density. Although the pole mass of σ decreases in the low density region, the screening mass behaves very differently from those of ρ at finite temperature and density. This difference is attributed to the corresponding Dirac- and Fermi-sea contributions.

TABLE I: Parameters of QHD-I determined at normal nuclear density $\rho_0 = 0.1484 fm^{-3}$. The masses are in (MeV).

g_σ^2	g_ω^2	m_σ	m_ω	$g_{\rho NN}$	k_ρ	m_ρ	M_N
54.289	102.770	458	783	2.63	6.1	770	939

Acknowledgments This work was supported by the NSFC under Grant Nos 10135030, 10175026, 19925519 and the China Postdoc Research Fund.

APPENDIX A

The ingredients of $\Pi_D^{\mu\nu}$ with the similar expressions of a and b in (9) are

$$\Pi_D^{00}(k) = \Pi_{1D}^{00} + \Pi_{2D}^{00} + \Pi_{3D}^{00},$$

$$\Pi_{1D}^{00} = -2\left(\frac{g_{\rho NN}}{2\pi}\right)^2 \int \frac{p^2 dp}{\omega}(n_B + \bar{n}_B) \left[4 + \frac{k^2 - 4\omega k_0 + 4\omega^2}{2p|\mathbf{k}|}a + (\omega \to -\omega)\right],$$

$$\Pi_{2D}^{00} = 4|\mathbf{k}|\left(\frac{g_{\rho NN}}{2\pi}\right)^2 \frac{k_\rho}{2M_N} M_N^* \int \frac{pdp}{\omega}(n_B + \bar{n}_B)(a+b),$$

$$\Pi_{3D}^{00} = 2\left(\frac{g_{\rho NN}}{2\pi}\right)^2 \left(\frac{k_\rho}{2M_N}\right)^2 \int \frac{p^2 dp}{\omega}(n_B + \bar{n}_B) \left[4k_0^2 + \frac{\mathbf{k}^2(k^2 - 4p^2) + (k^2 - 2k_0\omega)^2}{2p|\mathbf{k}|}a + (\omega \to -\omega)\right];$$

$$\Pi_D^{0i}(k) = \frac{k^0 k^i}{\mathbf{k}^2}\Pi_D^{00}(k);$$

$$\Pi_D^{ij}(k) = (A_1 + A_2 + A_3)\delta^{ij} + (B_1 + B_2 + B_3)\frac{k^i k^j}{\mathbf{k}^2},$$

$$A_1 = \left(\frac{g_{\rho NN}}{2\pi}\right)^2 \int \frac{p^2 dp}{\omega}(n_B + \bar{n}_B) \left[\frac{4(\mathbf{k}^2 + k_0^2)}{\mathbf{k}^2} - \frac{\mathbf{k}^4 - k_0^2(k_0 - 2\omega)^2 + 4\mathbf{k}^2(p^2 - k_0\omega)}{2p|\mathbf{k}|^3}a - (\omega \to -\omega)\right],$$

$$A_2 = \frac{k^2}{\mathbf{k}^2}\Pi_{2D}^{00},$$

$$A_3 = -k^2\left(\frac{g_{\rho NN}}{2\pi}\right)^2 \left(\frac{k_\rho}{2M_N}\right)^2 \int \frac{p^2 dp}{\omega}(n_B + \bar{n}_B) \left[\frac{4k^2}{\mathbf{k}^2} + \frac{k^4 + 4k^2\omega(\omega - k_0) + 4\mathbf{k}^2(p^2 - \omega^2)}{2p|\mathbf{k}|^3}a + (\omega \to -\omega)\right],$$

$$B_1 = \left(\frac{g_{\rho NN}}{2\pi}\right)^2 \int \frac{p^2 dp}{\omega}(n_B + \bar{n}_B) \left[-\frac{4(\mathbf{k}^2 + 3k_0^2)}{\mathbf{k}^2} + \frac{\mathbf{k}^4 - 3k_0^2(k_0 - 2\omega)^2 + 2\mathbf{k}^2(k_0^2 + 2p^2 - 2k_0\omega)}{2p|\mathbf{k}|^3}a + (\omega \to -\omega)\right],$$

$$B_2 = \Pi_{2D}^{00},$$

$$B_3 = \left(\frac{g_{\rho NN}}{2\pi}\right)^2 \left(\frac{k_\rho}{2M_N}\right)^2 \int \frac{p^2 dp}{\omega}(n_B + \bar{n}_B) \left[\frac{4(k_0^4 + k^4)}{\mathbf{k}^2} + \frac{k^2(2k_0^4 + k^4) + 4k_0 k^2(2k_0^2 + k^2)\omega - 4(2\mathbf{k}^2 + k^2)\mathbf{k}^2 p^2 + 4(2k_0^4 - k_0^2 k^2 + 2k^4)\omega^2}{2p|\mathbf{k}|^3} a + (\omega \to -\omega)\right].$$

[1] R. Rapp and J. Wambach, Adv. Nucl. Phys. **25**, 1 (2000).

[2] E.V. Shuryak, Phys. Lett. **B 78**, 150 (1978); K. Kajantie, J. Kapusta, L. McLerran and A. Mekjian, Phys. Rev. **D 34**, 2746 (1986); I. Tserruya, Nucl. Phys. **A 590**, 127c (1995).

[3] O. Teodorescu, A.K. Dutt-Mazumder and C. Gale, Phys. Rev. **C 63**, 034903 (2001); **66**, 015209 (2002); C. Song, P.W. Xia and C.M. Ko, *ibid.*, **52**, 408 (1995).

[4] C. Gale and J.I. Kapusta, Nucl. Phys. **B 357**, 65 (1991).

[5] T. Hatsuda and S.H. Lee, Phys. Rev. **C 46**, R34 (1992); S. Leupold, W. Peters and U. Mosel, Nucl. Phys. **A 628**, 311 (1997); F. Klingl, N. Kaiser and W. Weise, **A 624**, 527 (1997).

[6] G.E. Brown and M. Rho, Phys. Rev. Lett. **66**, 2720 (1991).

[7] G. Agakichiev *et al.*, CERES collaboration, Phys. Rev. Lett. **75**, 1272 (1995); P. Wurm, CERES collaboration, Nucl. Phys. **A 590**, 103c (1995).

[8] Guo-Qiang Li, C.M. Ko and G.E. Brown, Phys. Rev. Lett. **75**, 4007 (1995); Nucl. Phys. **A 606**, 568 (1996).

[9] J.I. Kapusta, *Finite Temperature Field Theory* (Cambridge University Press, Cambridge, England, 1989).

[10] S.A. Chin, Ann. Phys. **108**, 301 (1977).

[11] K. Saito, T. Maruyama and K. Soutome, Phys. Rev. **C 40**, 407 (1989); K. Saito and A. W. Thomas, *ibid.*, **51**, 2757 (1995).

[12] A. Rebhan, hep-ph/0111341.

[13] V.L. Eletsky, J.I. Kapusta and R. Venugopalan, Phys. Rev. **D 48**, 4398 (1993); M. Prakash, R. Rapp, J. Wambach and I. Zahed, Phys. Rev. **C 65**, 034906 (2002).

[14] G. Chanfray and M. Erickson, Eur. Phys. J.**A 16**, 291 (2003).

[15] H. Shiomi and T. Hatsuda, Phys. Lett. **B 334**, 281 (1994); T. Hatsuda, H. Shiomi and H. Kuwabara, Prog. Theor. Phys. **95**, 1009 (1996).

[16] Ji-sheng Chen, Jia-rong Li and Peng-fei Zhuang, J. High Energy Phys. **11**, 014 (2002).

[17] B.D. Serot and J.D. Walecka, Adv. Nucl. Phys. **16**, 1 (1986).

[18] R. Machleidt, K. Holinde and Ch. Elster, Phys. Rep. **149**, 1 (1987); R. Machleidt, Adv. Nucl. Phys. **19**, 189 (1989).

[19] H. Kurasawa and T. Suzuki, Nucl. Phys. **A 490**, 571 (1988).

[20] H.-C. Jean, J. Piekarewicz and A.G. Williams, Phys. Rev. **C 49**, 1981 (1994).

[21] A.K. Dutt-Mazumder, B. Dutta-Roy and A. Kundu, Phys. Lett. **B 399**, 196 (1997); S. Sarkar, J. Alam, P. Roy, A.K. Dutt-Mazumder, B. Dutt-Roy and B. Sinha, Nucl. Phys. **A 634**, 206 (1998).

[22] Y. Iwasaki, H. Kouno, A. Hasegawa and M. Nakano, Int. J. Mod. Phys. **E 9**, 459 (2000).

[23] J.C. Caillon and J. Labarsouque, Phys. Lett. **B 311**, 19 (1993).